

Supporting Information

**A New Mode of Chemical Reactivity for Metal-Free Hydrogen
Activation by Lewis Acidic Boranes**

*Elliot L. Bennett, Elliot J. Lawrence, Robin J. Blagg, Anna S. Mullen, Fraser MacMillan,
Andreas W. Ehlers, Daniel J. Scott, Joshua S. Sapsford, Andrew E. Ashley,*
Gregory G. Wildgoose,* and J. Chris Sootweg**

anie_201900861_sm_miscellaneous_information.pdf

Supporting Information

This PDF file includes:

Materials and Methods

X-ray crystallographic characterisation of compound **1**

Nuclear Magnetic Resonance Spectroscopic Data

Electrochemical Characterization of compound **1**

Figs. S1 to S14

Tables S1 to S2

DFT Data S1

Materials and Methods

Reagents and Equipment

All reactions and manipulations were performed under an inert atmosphere of dry, oxygen-free N₂, using either standard Schlenk techniques or in an MBraun UNILab glovebox, and kept in the dark by using reduced lighting in the laboratory and wrapping the vessels in foil throughout to prevent the possibility of adventitious photochemical reaction pathways. All solvents were dried prior to use by refluxing over an appropriate drying agent {Na/benzophenone for *n*-pentane, *n*-hexane, petroleum ether (b.p. 40–60 °C), diethyl ether and tetrahydrofuran (THF); Na for benzene and toluene; CaH₂ for dichloromethane and acetonitrile} collected by distillation under an inert N₂ atmosphere, and stored over 4 Å molecular sieves prior to use. Deuterated solvents (CD₂Cl₂ and THF-*d*₈) were freeze-pump-thaw degassed and stored over 3 Å molecular sieves. All glassware was flame-dried under vacuum before use. H₂ (99.995%, BOC Gases, UK) and D₂ (99.995% CK Special Gases Ltd, UK) were dried by passage through a drying column containing P₂O₅. Unless stated otherwise all other reagents were purchased from commercial suppliers and used as received.

NMR spectra were obtained on a Bruker Advance DPX-500 spectrometer; ¹H and ¹³C spectra were referenced internally to residual solvent signals, whilst for ¹¹B spectra BF₃·Et₂O was used as an external standard. 500 MHz NMR tubes (Norrel) sealed with a J Young valve were used throughout to maintain the desired N₂, H₂, or D₂ atmospheres.

EPR spectra were obtained on a Bruker eleXsys E500 spectrometer using a standard rectangular Bruker EPR cavity (4102ST). Samples were measured in standard 4mm quartz EPR tubes (WilmaD) fitted with J Young valves to maintain the desired atmospheres. Experimental parameters: microwave power, 20 mW (figures 3A, 3B, 3D) and 0.8 mW (figure 3C); field modulation frequency, 100 kHz; field modulation amplitude, 0.1 mT (figures 3A-C) and 0.2 mT (figure 3D); all performed at ambient room temperature. All spectral simulations were performed using the MATLAB-based EasySpin package¹.

Infra-red spectra were obtained using a PerkinElmer Spectrum Two FT-IR spectrometer; samples were recorded using an attenuated total reflectance (ATR) module or in a Nujol mull on NaCl discs.

Mass spectrometry was performed by the EPSRC Mass Spectrometry Service at the University of Swansea. Elemental analyses were performed by the Elemental Analysis Service at London Metropolitan University.

Single crystals of **1** were grown by slow evaporation of a CH₂Cl₂ solution; data collection and processing was performed at the UK National Crystallographic Service at the University of Southampton². Using Olex2³, the structure was solved and space group assigned with ShelXS version 2014/7⁴ using direct methods, and then refined with the ShelXL version 2014/7⁴ refinement program using least squares minimisation.

CCDC 1502851 contains the supplementary crystallographic data for this paper. These data can be obtained free of charge from The Cambridge Crystallographic Data Centre *via* www.ccdc.cam.ac.uk/data_request/cif.

Preparation of samples for NMR experiments

Compound **1**: Inside the glovebox 12 mg (19 μmol) of **1** was dissolved in either CD₂Cl₂ or THF-*d*₈ in the NMR tube and 6.2 mg (19 μmol) of Cp*₂Co (Cp* = pentamethylcyclopentadienyl, (CH₃)₅C₅⁻) added. The solutions turned a deep purple/red

(CD₂Cl₂) or and orange/brown color (THF-d₈). H₂ was admitted via a sequence of three freeze-pump-thaw cycles. The reaction mixture was then heated in the dark at 50 °C or 65 °C respectively, and monitored periodically via multinuclear NMR spectroscopy. For experiments using D₂ the same procedure was observed except the solvents were replaced with their *protio* analogues.

Compound **2**: Inside the glovebox 40 mg (0.109 mmol) of **2** was dissolved in THF-d₈ and 45 mg (an excess, 2.0 mmol, 18 equivalents) of sodium metal added. The solutions turned a deep blue color. The solution was filtered through a glass wool plug into an NMR tube. H₂ was admitted via a sequence of three freeze-pump-thaw cycles. The reaction mixture was then heated in the dark at 65 °C respectively, and monitored periodically via multinuclear NMR spectroscopy. For experiments using D₂ the same procedure was observed except the solvent was replaced with *protio*-THF.

Preparation of samples for EPR experiments

Inside the glovebox a 5 μM solution of **1** in either CD₂Cl₂ or THF-d₈ was reduced by adding an excess (3 molar equivalents) of Cp*₂Co in a glass vial. The reaction mixture was briefly stirred before the solution was filtered (by pipetting through a glass wool plug to remove any residual reducing agent/solid) into a 4mm quartz EPR tube fitted with a J Young valve. EPR spectra were recorded for each sample before H₂ was admitted via a sequence of three freeze-pump-thaw cycles. The EPR spectra were recorded again after addition of H₂ to the reaction mixture, and then the reaction mixtures were heated in the dark at 50 °C (CD₂Cl₂) or 65 °C (THF-d₈) with periodic monitoring by EPR spectroscopy (see main text).

Density Functional Theory Computational Methods

Density functional calculations were performed at the ωB97X-D⁵ level of theory using Gaussian09, revision D.01.⁶ Geometry optimizations were performed using the 6-31G(d,p) basis set⁷⁻¹⁷ and uncorrected energies were obtained from single point calculations using the 6-311G(d,p) basis set.^{5,17-20} Loose criteria for the geometry optimizations have been applied due to the smooth topology of the potential energy surfaces caused by the presence of the nine methyl groups. The resulting data are given listed in Data S1.

Table S1. Calculated energies for the reaction step: Ar₃B + H[•] → [Ar₃B-H][•] with the hydrogen atom located at both the boron atom and at different positions around the aryl ring system in [Ar₃B-H][•].

Compound	Energy for hydrogen atom at different positions in [Ar ₃ B-H] [•] (kcal mol ⁻¹)				
	Boron	<i>ipso</i> -C	<i>ortho</i> -C	<i>meta</i> -C	<i>para</i> -C
1	No stable structure	-34.1	-37.6	-37.7	-37.8
2	-7.9*	-28.9	-29.5	-32.1	-31.3

* Only optimizable if C₃ symmetry is forced upon the simulated structure.

Electrochemical methods

Electrochemical studies were carried out using a Metrohm Autolab PGSTAT30 potentiostat linked to a computer running Metrohm Autolab NOVA version 1.11 software, in conjunction with an inert atmosphere three-electrode cell (in house design). The working electrode was a

glassy carbon disc (Bioanalytical Systems, Inc., $\approx 7.0 \text{ mm}^2$ area calibrated using the $[\text{FeCp}_2]^{0/+}$ redox couple); the counter electrode was a platinum wire (99.99% purity); and the *pseudo*-reference electrode a silver wire (99.99% purity). The GCE was polished between experiments using successive grades of diamond paste slurries from 3.0 to 0.1 μm (Kemet, Maidstone, UK), sonicated in ethanol between each grade of polishing material and dried under a stream of N_2 . All electrochemical measurements (cyclic voltammetry) were performed at ambient temperature under a dry/solvent saturated N_2 atmosphere, in CH_2Cl_2 or THF as appropriate containing 0.05 M $[\text{nBu}_4\text{N}][\text{B}(\text{C}_6\text{F}_5)_4]$ as the supporting electrolyte. All potentials were referenced to the $[\text{FeCp}_2]^{0/+}$ redox couple, which was added as an internal standard at the end of each experiment.

Synthesis

The synthesis of tris(3,5-dinitromesityl)borane, compound **1**, from tris(mesityl)borane, compound **2**, was achieved by adapting the method of Hawkins *et al.*²¹. In contrast to the highly cited literature method of Brown and Dodson²² for the preparation of **2**, via a Grignard reagent, we report an improved method using a mesityllithium reagent (LiMes). The air and moisture sensitive LiMes reagent can be safely isolated on >20g scale and did not decompose over periods of several months when stored under an inert atmosphere. The LiMes preparative route to make **2** results in an improved overall reaction yield (68%) compared to the standard Grignard literature method (49%),²³ avoids the need to change solvents (Et_2O /toluene) multiple times, and to perform organic/aqueous separations to remove the magnesium salt by-products.

Mesityllithium (LiMes)

This compound was made by a modification of a literature procedure.²⁴ Bromomesitylene (15 mL, 98.02 mmol) was dissolved in diethyl ether (Et_2O) (300 mL) and cooled to 0 °C. nBuLi (50.97 mL, 127.43 mmol, 2.5 M in hexanes) was added and the reaction mixture stirred at room temperature for 72 hours. The mixture was then allowed to settle, filtered via cannula, the white solid washed with cold *n*-pentane (2 x 150 mL) and then dried under vacuum to yield mesityllithium as a white free flowing solid (9.82 g, 77.86 mmol, 79%).

^1H NMR (500 MHz, toluene- d_8 , 298 K): 6.67 (2H, s, *meta*-H), 2.25 (3H, s, *para*-Me), 2.15 (6H, s, *ortho*-Me).

Tris(mesityl)borane (Compound 2)

LiMes (5.00 g, 39.64 mmol) was suspended in toluene (200 mL) and BCl_3 (11.49 mL, 11.49 mmol, 1 M in heptane) was added dropwise. The reaction mixture was heated under reflux for 2.5 hours before being allowed to cool to room temperature. The resulting brown suspension was filtered and the yellow toluene filtrate retained. The solvent was removed under reduced pressure and the crude off-white solid dried under dynamic vacuum. The crude solid was re-crystallised twice from ethanol (EtOH) to yield **2** as a pure white solid. The mother liquor was concentrated to approximately 1/3 of the initial volume and filtered to recover a further 0.3 g of the pure product, **2**. (3.64 g, 9.88 mmol, 86%).

^1H NMR (500 MHz, C_6D_6 , 298 K): 6.72 (6H, s, *meta*-H), 2.15 (18H, s, *ortho*-Me), 2.14 (9H, s, *para*-Me);

^{11}B NMR (160 MHz, C_6D_6 , 298 K): 76.59 (br s);

$^{13}\text{C}\{^1\text{H}\}$ NMR (126 MHz, C_6D_6 , 298 K): 144.85 (*para*-C), 140.81 (*ortho*-C), 139.43 (*ipso*-C), 129.27 (*meta*-C), 23.17 (*ortho*-Me), 21.31 (*para*-Me).

Tris(3,5-dinitromesityl)borane (Compound 1) ²¹

A mixture of white fuming HNO₃ (28 mL) and conc. H₂SO₄ (16 mL) was cooled to -70 °C and stirred using a mechanical overhead stirrer. Compound **2** (2.00 g, 5.43 mmol) was added in small portions over 15 minutes, upon which the thick paste like mixture turned a light brown colour. The reaction was stirred at -70 °C for 1 hour and then allowed to slowly warm to -40 °C over a period of 90 minutes, after which H₂O (60 mL) was carefully added. The mixture was stirred for 10 minutes and then filtered through a glass sinter (medium G02 porosity). The solid residue was washed with copious amounts of H₂O and air-dried under reduced pressure for 1 h. The crude off-white solid was recrystallized from ethyl acetate, filtered, and then dried under dynamic vacuum at 60 °C for 45 minutes to yield pure **1** as a cream coloured free-flowing powder (2.18 g, 3.41 mmol, 63%).

¹H NMR (500 MHz, CD₂Cl₂, 298 K): 2.24 (9H, s, *para*-Me), 2.04 (18H, s, *ortho*-Me);

¹¹B NMR (160 MHz, CD₂Cl₂, 298 K): 75.08 (br s);

¹³C{¹H} NMR (125 MHz, CD₂Cl₂, 298 K): 152.30 (*meta*-C), 145.68 (*ipso*-C), 133.13 (*ortho*-C), 125.79(*para*-C), 18.36 (*ortho*-Me), 13.60 (*para*-Me);

FTIR (Neat - ATR): $\tilde{\nu}$ / cm⁻¹ = 1525 (N-O asymmetric stretch), 1355 (N-O symmetric stretch);

HRMS-APCI (*m/z*): [C₂₇H₂₈B₁N₆O₁₂]⁺ as [M + H]⁺: calc. 639.1858, observed 639.1865;

Elemental analysis (calc. for C₂₇H₂₇BN₆O₁₂): C 50.89 (50.80), H 4.09 (4.26), N 12.97 (13.17).

Sodium tris(3,5-dinitromesityl)borohydride ([Na][1-H])

Compound **1** (0.50 g, 0.78 mmol) was dissolved in anhydrous CH₂Cl₂ (30 mL) and [Na][HBEt₃] (0.78 mL, 0.78 mmol, 1 M in toluene) was slowly added dropwise. The reaction mixture immediately turned blue (indicative of a single electron transfer side reaction to produce blue **1**⁻ impurities. This SET side reaction is commonly observed in our laboratories when treating sterically hindered triaryl boranes with [Na][HBEt₃]), and was left to stir for 12 hours. The solvent was removed under reduced pressure, and the impure blue solid was eluted through a small plug of silica using CH₂Cl₂ followed by CH₃CN. The CH₃CN fractions were collected, the solvent was removed under reduced pressure, and the resulting solid dried under dynamic vacuum to yield [Na][**1**-H] as a red/brown powder with high purity.

¹H NMR (500 MHz, CD₃CN, 298 K): 3.80 (1H, br q, J_{HB} = 80.7 Hz, HB), 2.05 (9H, s, *para*-Me), 1.91 (9H, br s, *ortho*-Me), 1.76 (9H, br s, *ortho*-Me);

¹¹B NMR (160 MHz, CD₃CN, 298 K): -13.28 (d, J_{BH} = 80.7 Hz);

¹³C{¹H} NMR (126 MHz, CD₃CN, 298 K): 150.63, 133.48, 128.60, 127.90, 115.19, 114.52 (aromatic C), 17.70 (*ortho*-Me), 16.21 (*ortho*-Me), 11.27 (*para*-Me);

FTIR (Neat - ATR): $\tilde{\nu}$ / cm⁻¹ = 1514 (N-O asymmetric stretch), 1354 (N-O symmetric stretch);

HRMS-NSI (*m/z*): [M - Na]⁻ or [C₂₇H₂₈BN₆O₁₂]⁻, calc. 639.1869, observed 639.1840;

Elemental analysis (calc. for C₂₇H₂₈BN₆NaO₁₂·2H₂O): C 46.17 (46.44), H 4.67 (4.62) N 11.71 (12.03).

X-ray crystallographic characterisation of compound 1

An X-ray crystal structure was obtained from a single crystal of **1**, grown by the slow evaporation of a concentrated CH₂Cl₂ solution at room temperature (Fig. S1-S2, Table S1.)

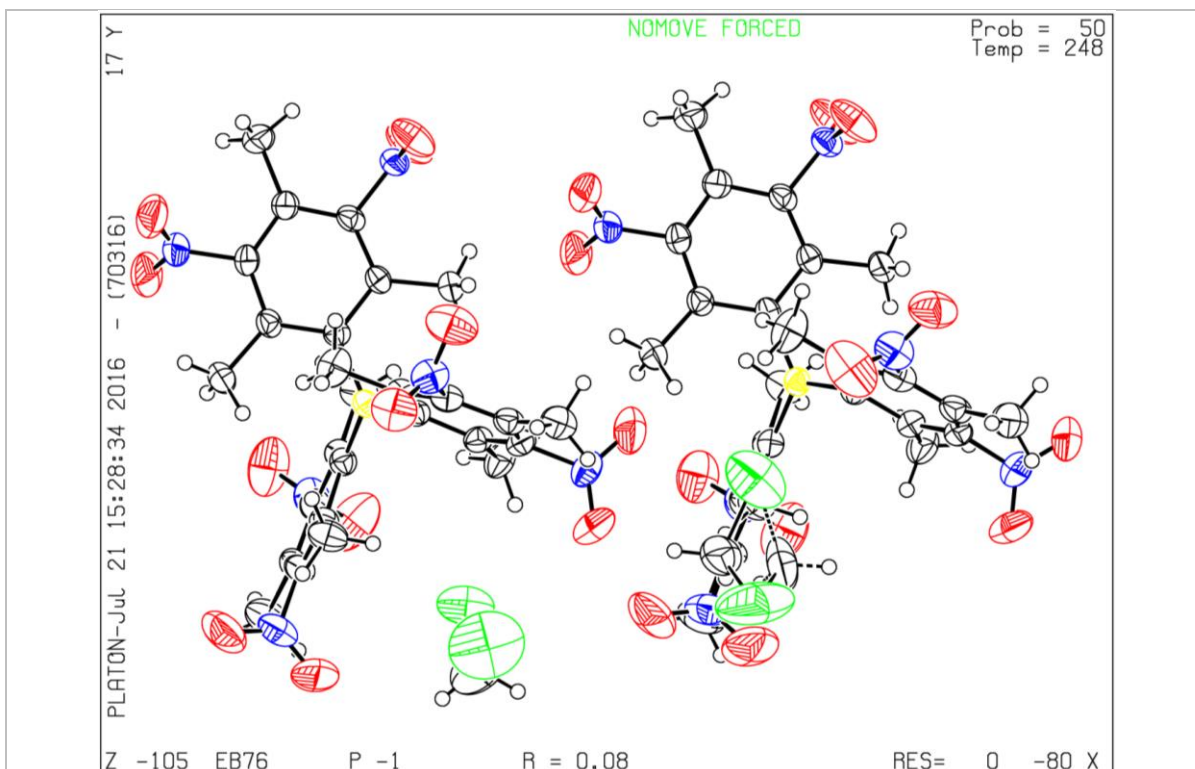


Fig. S1. X-ray crystallographic structure of compound **1**.

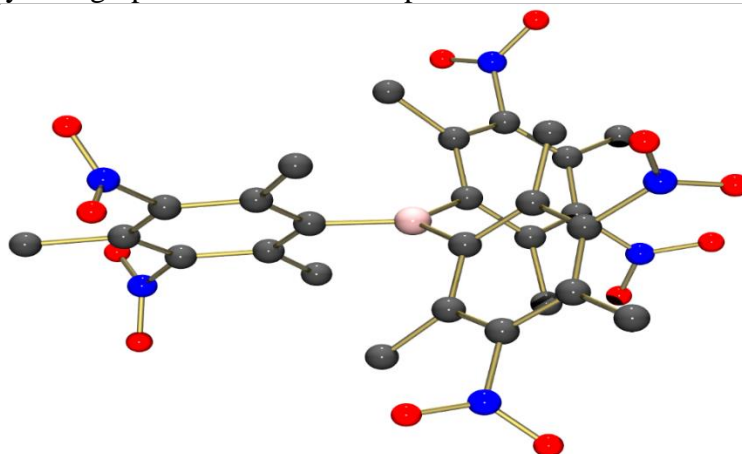


Fig. S2. Ball and stick render of one of the two independent molecules of compound **1** found in the asymmetric unit cell (hydrogen atoms removed for clarity).

The asymmetric unit comprised two crystallographically unique molecules of **1**, with negligible differences in structural metrics between them, along with two molecules of CH_2Cl_2 . The structure of **1** is consistent with previous reports for tri(aryl)boranes, including that of **2**,^{23,24} with a trigonal planar boron centre and the three aryl rings twisted with respect to the trigonal plane minimising steric clash between them. The twist for the aryl rings in **1**, $51(3)^\circ$, is comparable to that of **2**, $50(2)^\circ$, indicating poor orbital overlap between the aromatic π -orbitals and the formally vacant boron p_z orbital. The nitro-substituents are perpendicular to the aromatic ring to which they are bound. As with **2**, the interlocking *ortho*-methyl substituents of **1** surround the boron-centre, sterically shielding the formally Lewis acidic site from reacting with Lewis bases.

Table S2. Crystallographic data for compound **1**·CH₂Cl₂

	1 ·CH ₂ Cl ₂
Empirical formula	C ₂₈ H ₂₉ BCl ₂ N ₆ O ₁₂
Formula weight	723.28
Temperature / K	248(2)
Crystal system	triclinic
Space group	P-1
<i>a</i> / Å	13.3197(3)
<i>b</i> / Å	14.8658(4)
<i>c</i> / Å	18.2003(5)
α / °	104.670(2)
β / °	106.133(2)
γ / °	92.184(2)
Volume / Å ³	3326.14(16)
<i>Z</i>	4
ρ_{calc} g/cm ³	1.444
μ / mm ⁻¹	0.266
F(000)	1496.0
Crystal size / mm ³	0.138 × 0.097 × 0.032
Radiation	Mo <i>K</i> α (λ = 0.71073 Å)
2 Θ range for data collection	3.194 to 54.97°
Index ranges	-17 ≤ <i>h</i> ≤ 17, -19 ≤ <i>k</i> ≤ 19, -23 ≤ <i>l</i> ≤ 21
Reflections collected	45312
Independent reflections	15143 [R _{int} = 0.0373, R _{sigma} = 0.0504]
Data / restraints / parameters	15143 / 0 / 911
Goodness-of-fit on F ²	1.039
Final R indexes [$I \geq 2\sigma(I)$]	R ₁ = 0.0829, wR ₂ = 0.2240
Final R indexes [all data]	R ₁ = 0.1392, wR ₂ = 0.2649
Largest diff. peak / hole / e.Å ⁻³	0.69 / -0.80

Nuclear Magnetic Resonance Spectroscopic Data

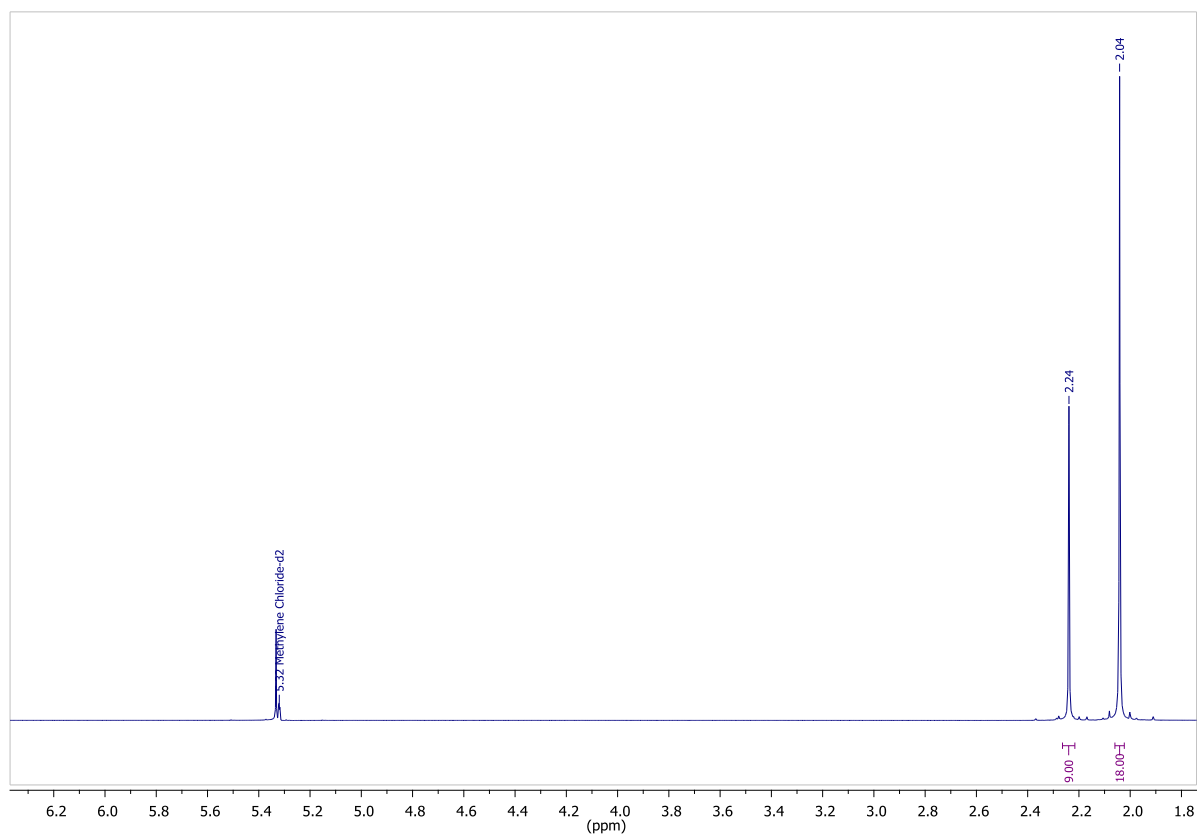


Fig. S3. ^1H NMR of **1** in CD_2Cl_2 .

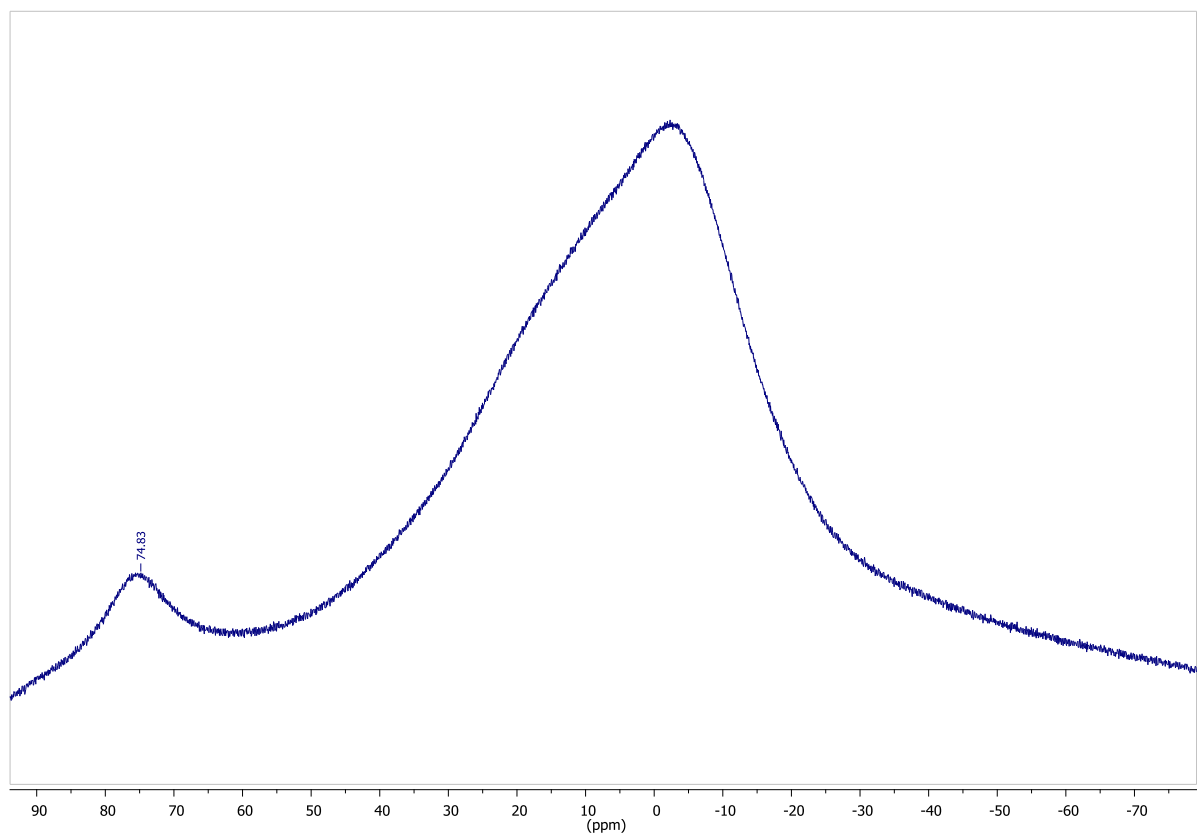


Fig. S4. ^{11}B NMR of **1** in CD_2Cl_2 .

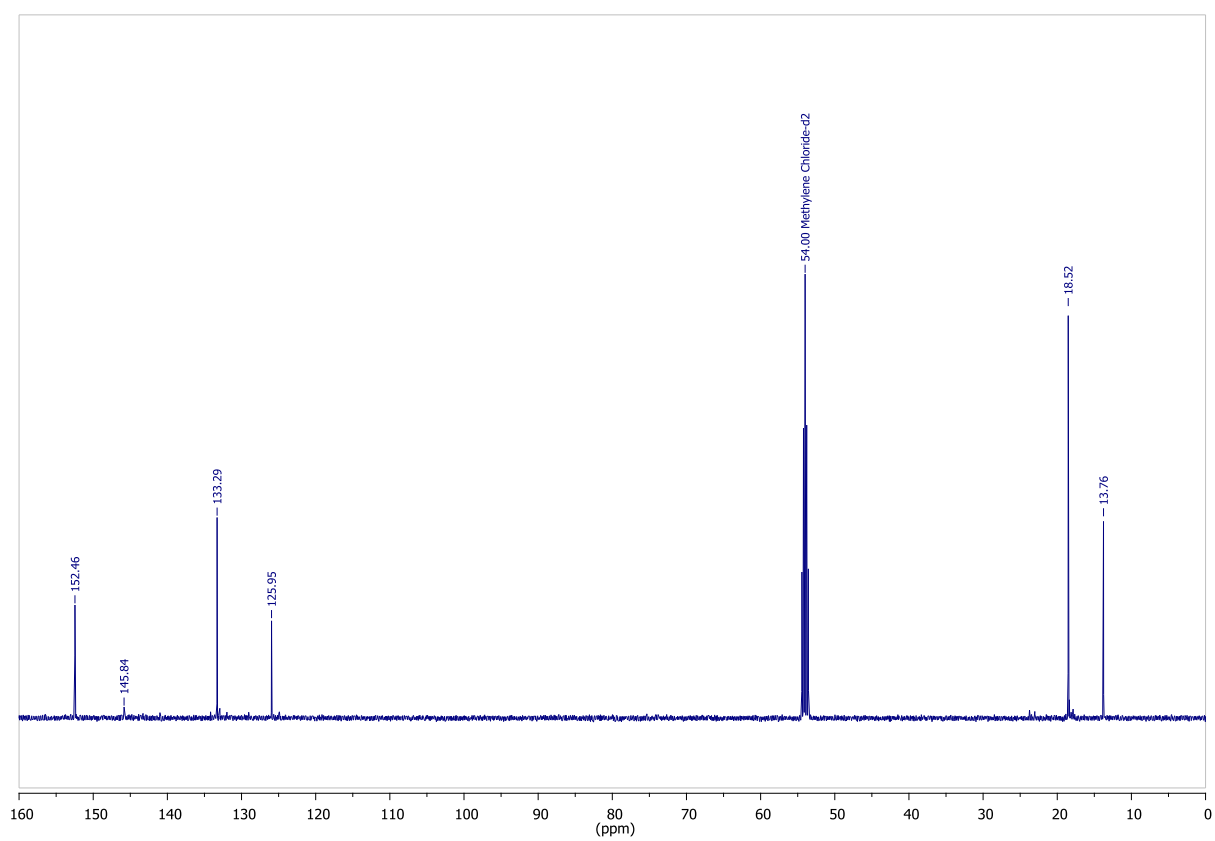


Fig. S5. $^{13}\text{C}\{^1\text{H}\}$ NMR of **1** in CD_2Cl_2 .

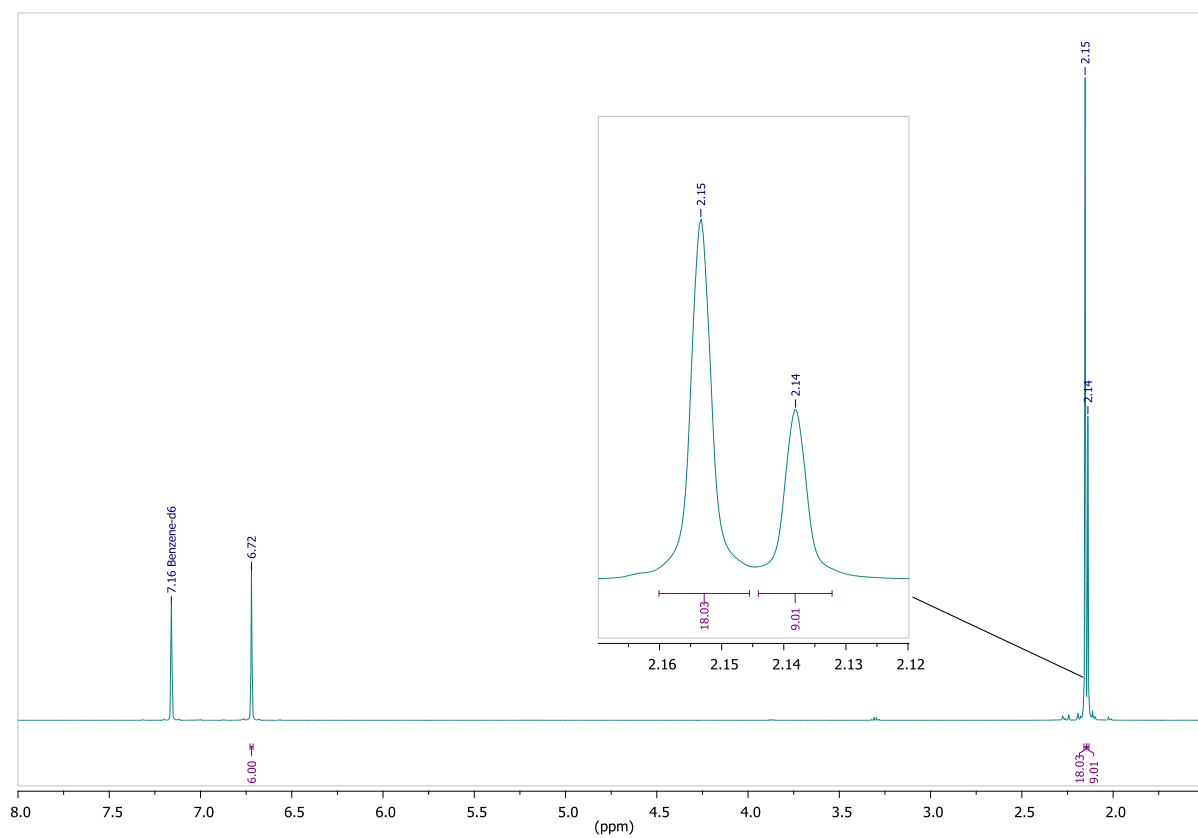


Figure S6. ^1H NMR of **2** in C_6D_6 .

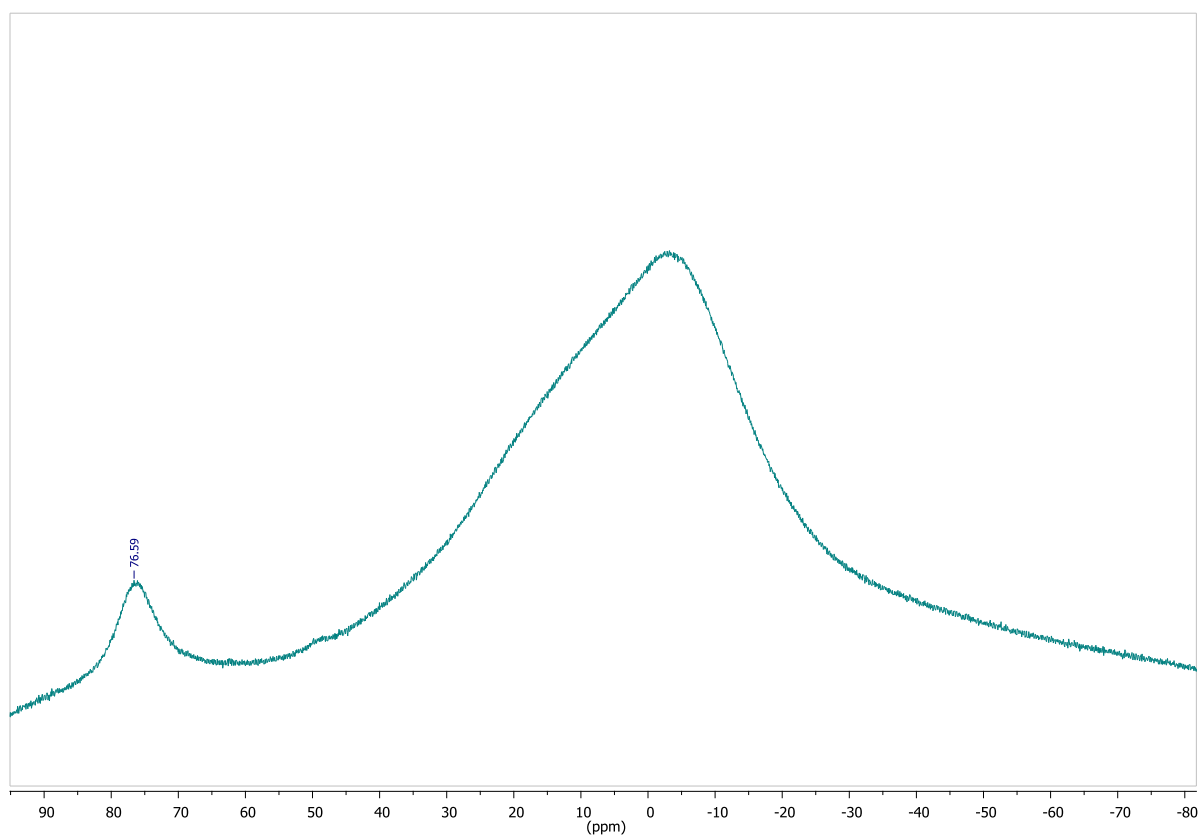


Fig. S7. ^{11}B NMR of **2** in C_6D_6 .

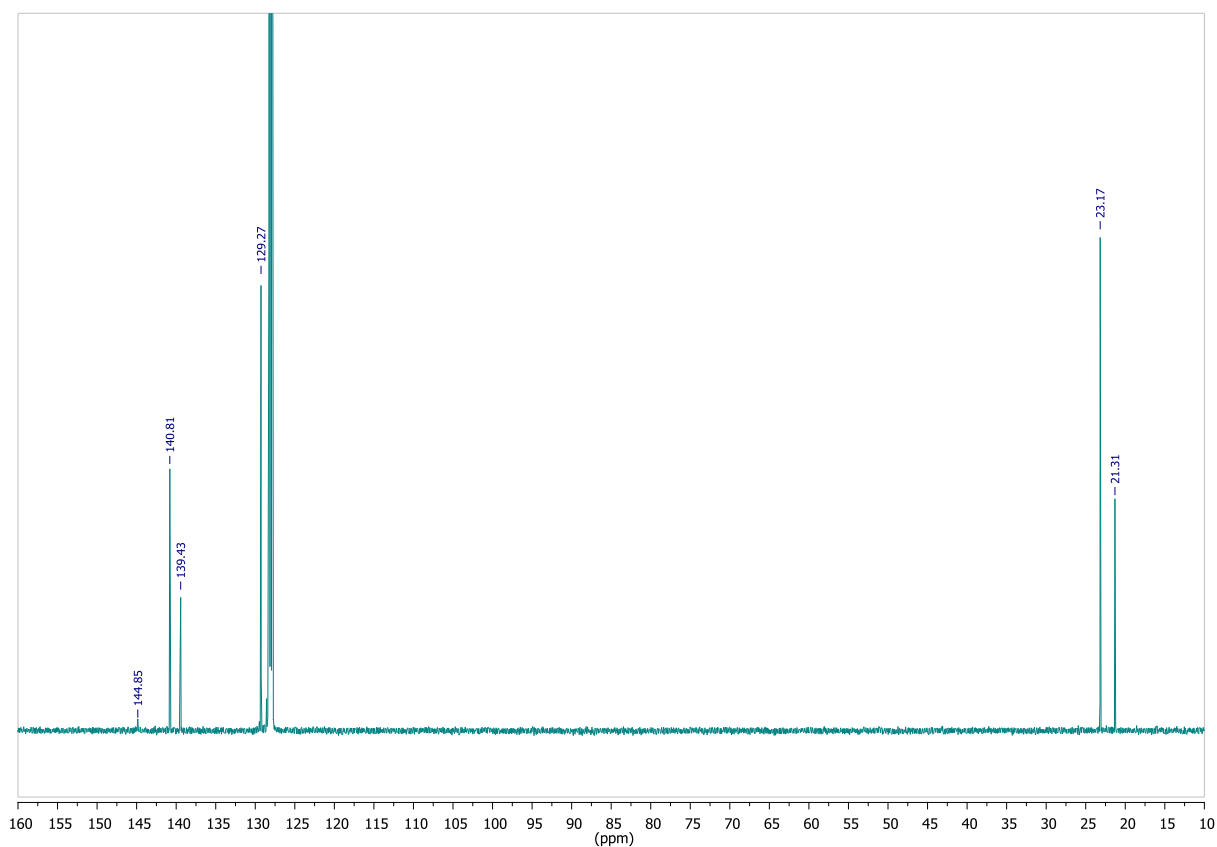


Fig. S8. $^{13}\text{C}\{^1\text{H}\}$ NMR of **2** in C_6D_6 .

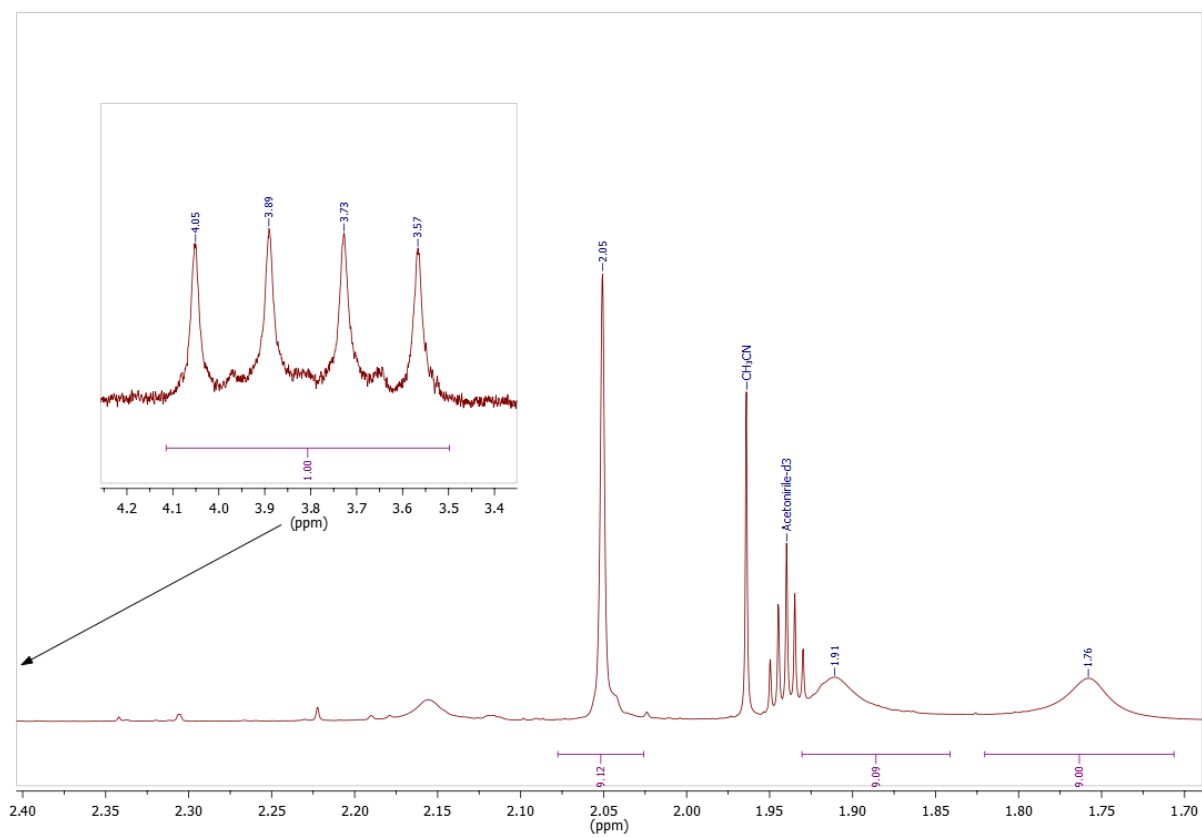


Fig. S9. ^1H NMR of $[\text{Na}][\mathbf{1-H}]$ showing broadening/separation of Me signals in CD_3CN .

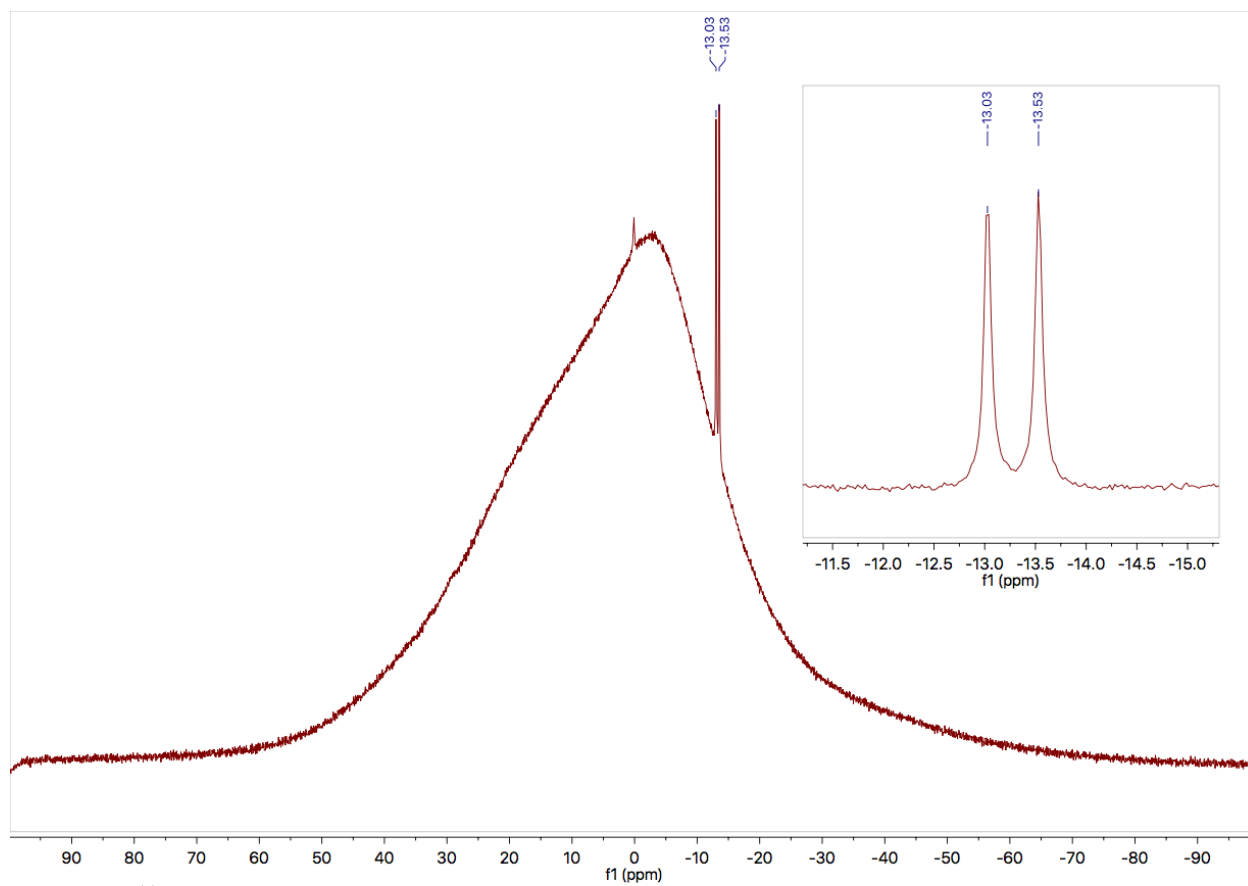


Fig. S10. ^{11}B NMR of $[\text{Na}][\mathbf{1-H}]$

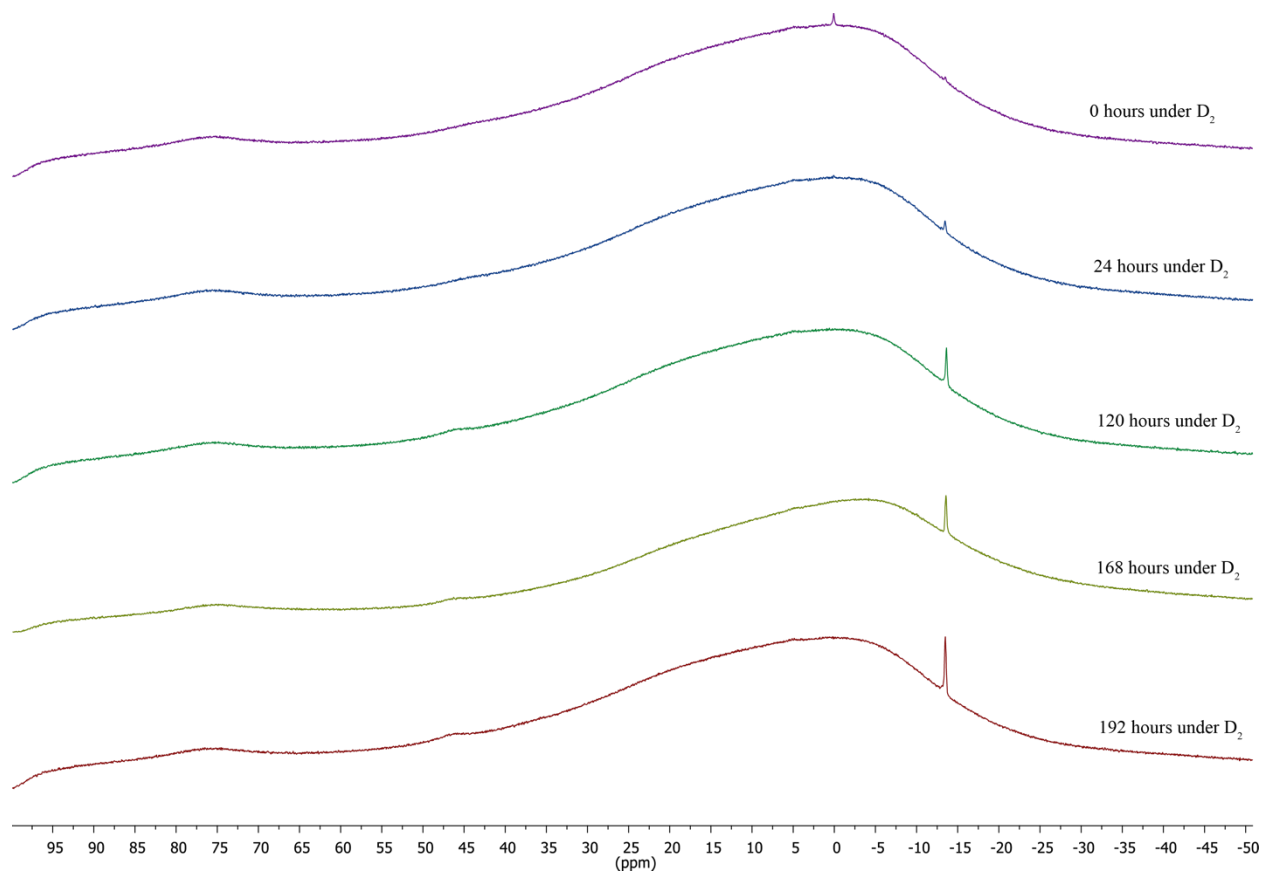


Fig S11. ^{11}B NMR showing the progress of D_2 cleavage by **1** in CH_2Cl_2 .

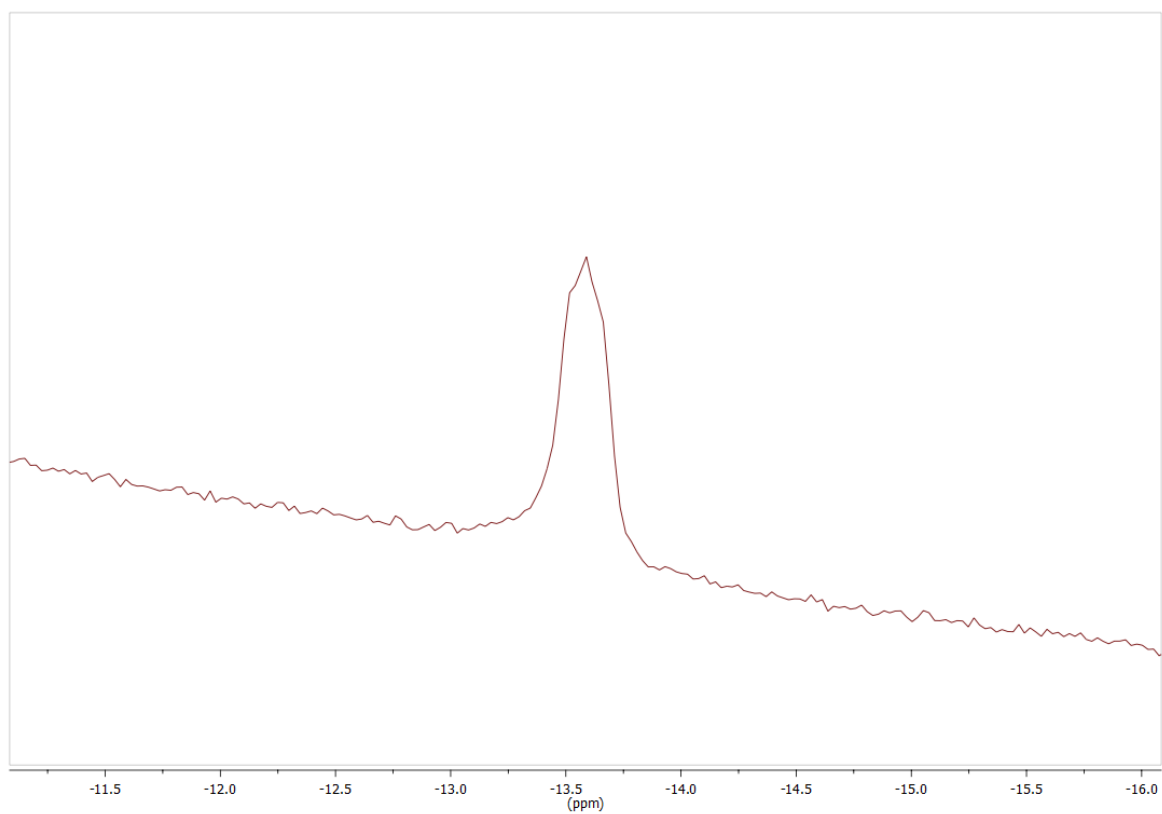


Fig S12. An expanded view of the $[1\text{-D}]^-$ region from Fig. S11 above after 192 hours.

Electrochemical Characterization of Compound 1

Electrochemical characterization of compound **1** was performed in both CH₂Cl₂ and THF electrolyte solutions. Upon first scanning in a reductive direction three quasi-reversible redox peaks are observed (Fig S13), corresponding to the reduction of the borane (Peak I) and the sequential reduction of the aromatic NO₂ groups (Peaks II and III) assigned by comparison to the voltammetric response of 3,5-dinitromesitylene.

Variable scan rate experiments (Fig S14) confirmed the quasi-reversible nature of the borane reduction wave, especially when the scan was reversed prior to the reduction of the NO₂ groups. The borane reduction was much less reversible in CH₂Cl₂ than THF, consistent with the NMR results in the main text which indicate that the radical anion intermediate interacts with halogenated solvents (*via* an EC process in Testa–Reinmuth notation).

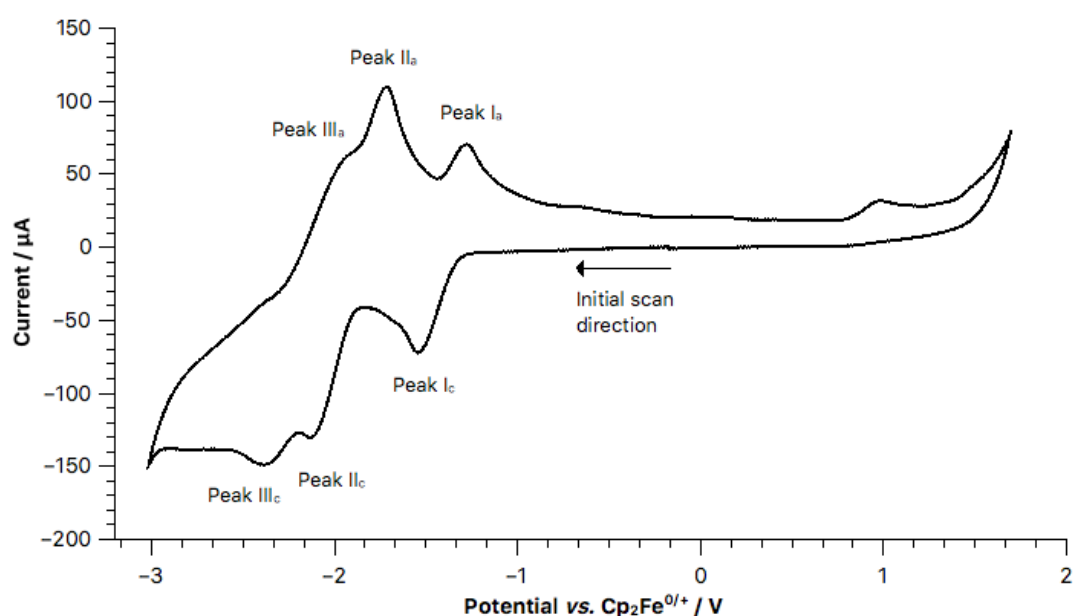


Fig S13. Cyclic voltammogram recorded for compound **1** (2.0 mM in THF containing 0.05 M [ⁿBu₄N][B(C₆F₅)₄] as the supporting electrolyte) recorded at a voltage scan rate of 200 mVs⁻¹.

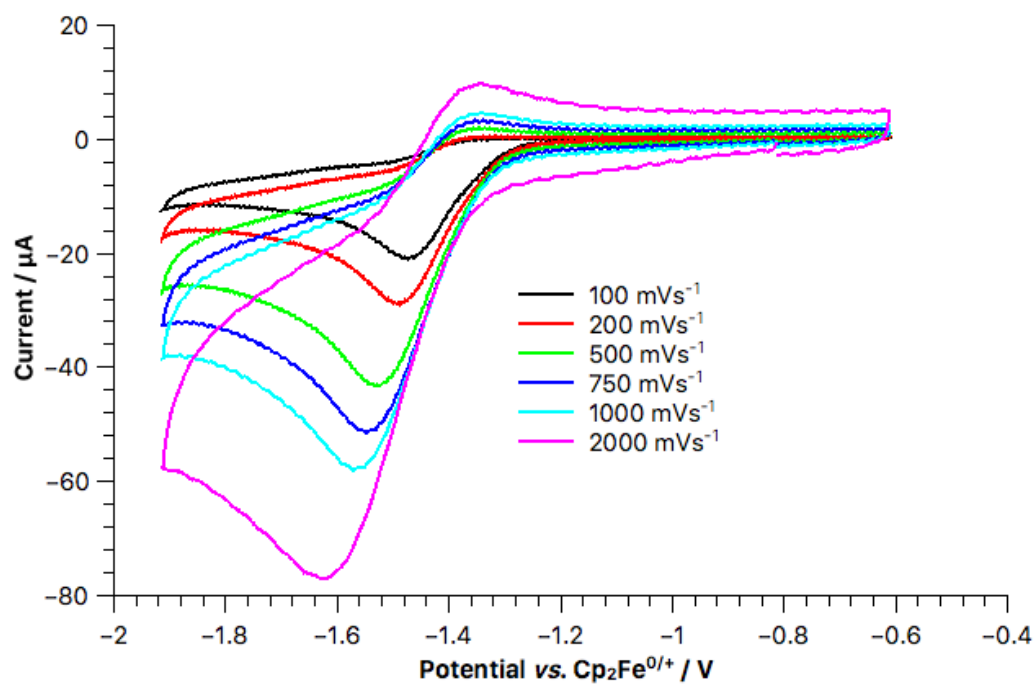


Fig S14. Overlaid cyclic voltammograms recorded for compound **1** (2.0 mM in CH_2Cl_2 containing 0.05 M $[\text{nBu}_4\text{N}][\text{B}(\text{C}_6\text{F}_5)_4]$ as the supporting electrolyte) recorded at different voltage scan rates over the voltage region corresponding to the reduction of the borane.

References

- 1 S. Stoll, A. Schweiger, EasySpin, a comprehensive software package for spectral simulation and analysis in EPR. *J Magn Reson.* **2006**, *178*, 42-55.
- 2 S. J. Coles, P. A. Gale, Changing and challenging times for service crystallography. *Chem. Sci.* **2012**, *3*, 683-689.
- 3 O. V. Dolomanov, L. J. Bourhis, R. J. Gildea, J. A. K. Howard, H. Puschmann, OLEX2: a complete structure solution, refinement and analysis program. *J. Appl. Cryst.* **2009**, *42*, 339-341.
- 4 G. M. Sheldrick, A short history of SHELX. *Acta Crystallogr. A* **2008**, *64*, 112-122.
- 5 J.-D. Chai, M. Head-Gordon, Long-range corrected hybrid density functionals with damped atom-atom dispersion corrections. *Phys. Chem. Chem. Phys.* **2008**, *10*, 6615-6620.
- 6 M. J. Frisch, *et al.* Gaussian 09, Revision D.01. (Wallingford CT, 2013).
- 7 R. Ditchfield, W. J. Hehre, J. A. Pople, Self-Consistent Molecular-Orbital Methods .9. Extended Gaussian-Type Basis for Molecular-Orbital Studies of Organic Molecules. *J. Chem. Phys.* **1971**, *54*, 724-728.
- 8 W. J. Hehre, R. Ditchfield, J. A. Pople, Self-Consistent Molecular-Orbital Methods .12. Further Extensions of Gaussian-Type Basis Sets for Use in Molecular-Orbital Studies of Organic-Molecules. *J. Chem. Phys.* **1972**, *56*, 2257-2261.
- 9 P. C. Hariharan, J. A. Pople, Influence of Polarization Functions on Molecular-Orbital Hydrogenation Energies. *Theoret. Chim. Acta* **1973**, *28*, 213-222.
- 10 P. C. Hariharan, J. A. Pople, Accuracy of Ah Equilibrium Geometries by Single Determinant Molecular-Orbital Theory. *Mol. Phys.* **1974**, *27*, 209-214.
- 11 M. S. Gordon, The Isomers of Silacyclopropane. *Chem. Phys. Lett.* **1980**, *76*, 163-168.
- 12 M. M. Francl, *et al.* Self-Consistent Molecular-Orbital Methods .23. A Polarization-Type Basis Set for 2nd-Row Elements. *J. Chem. Phys.* **1982**, *77*, 3654-3665.
- 13 R. C. Binning, L. A. Curtiss, Compact Contracted Basis-Sets for 3rd-Row Atoms - Ga-Kr. *J. Comput. Chem.* **1990**, *11*, 1206-1216.
- 14 J. P. Blaudeau, M. P. McGrath, L. A. Curtiss, L. Radom, Extension of Gaussian-2 (G2) theory to molecules containing third-row atoms K and Ca. *J. Chem. Phys.* **1997**, *107*, 5016-5021.
- 15 V. A. Rassolov, J. A. Pople, M. A. Ratner, T. L. Windus, 6-31G* basis set for atoms K through Zn. *J. Chem. Phys.* **1998**, *109*, 1223-1229.
- 16 V. A. Rassolov, M. A. Ratner, J. A. Pople, P. C. Redfern, L. A. Curtiss, 6-31G*basis set for third-row atoms. *J. Comput. Chem.* **2001**, *22*, 976-984.
- 17 M. J. Frisch, J. A. Pople, J. S. Binkley, Self-Consistent Molecular-Orbital Methods .25. Supplementary Functions for Gaussian-Basis Sets. *J. Chem. Phys.* **1984**, *80*, 3265-3269.
- 18 R. Krishnan, J. S. Binkley, R. Seeger, J. A. Pople, Self-Consistent Molecular-Orbital Methods .20. Basis Set for Correlated Wave-Functions. *J. Chem. Phys.* **1980**, *72*, 650-654.
- 19 A. D. Mclean, G. S. Chandler, Contracted Gaussian-Basis Sets for Molecular Calculations .1. 2nd Row Atoms, Z=11-18. *J. Chem. Phys.* **1980**, *72*, 5639-5648.
- 20 T. Clark, J. Chandrasekhar, G. W. Spitznagel, P. V. Schleyer, Efficient Diffuse Function-Augmented Basis Sets for Anion Calculations. Iii. The 3-21+G Basis Set for First-Row Elements, Li-F. *J. Comput. Chem.* **1983**, *4*, 294-301.

- 21 R. T. Hawkins, W. J. Lennarz, H. R. Snyder, Arylboronic Acids. V. Methyl-substituted Boronic Acids, Borinic Acids and Triarylborons^{1,2}. *J. Am. Chem. Soc.* **1960**, *82*, 3053-3059.
- 22 H. C. Brown, V. H. Dodson, Studies in Stereochemistry. XXII. The Preparation and Reactions of Trimesitylborane. Evidence for the Non-localized Nature of the Odd Electron in Triarylborane Radical Ions and Related Free Radicals¹. *J. Am. Chem. Soc.* **1957**, *79*, 2302-2306.
- 23 J. F. Blount, P. Finocchiaro, D. Gust, K. Mislow, Conformational analysis of triarylboranes. *J. Am. Chem. Soc.* **1973**, *95*, 7019-7029.
- 24 M. M. Olmstead, P. P. Power, First structural characterization of a boron-centered radical: x-ray crystal structure of [Li(12-crown-4)₂]⁺ [BMes₃]⁻. *J. Am. Chem. Soc.* **1986**, *108*, 4235-4236.